The use of a thiadiazole derivative to inhibit mild steel corrosion in 1 M HCl solution: Electrochemical and surface active aspects

M.D. Plotnikova,* M.G. Shcherban, A.B. Shein, A.S. Sofronov and P.G. Melnikov

Perm State National Research University, st. Bukireva 15, 614068, Perm, Russian Federation
**E-mail: plotnikova-md@mail.ru*

Abstract

Some aspects of mild steel corrosion in 1 M hydrochloric acid with addition of 1,3-DPTA in the corrosive system were studied by weight loss and electrochemical methods (potentiodynamic polarization measurements and electrochemical impedance spectroscopy) and also by contact angle and surface tension measurements. *N*-(1,3-dithiolan-2-ylidene)-5-phenyl-1,3,4-thiadiazole-2-amine (1,3-DPTA) has high inhibitory effect on the cathodic and anodic reactions on steel in HCl solutions. To determine the mechanism of inhibition of 1,3-DPTA, different adsorption isotherms including Langmuir, Freundlich, Temkin and Redlich-Peterson model were studied. The adsorption of 1,3-DPTA is described as a complex process of interaction of inhibitor molecules with the steel surface linearized in the coordinates $\ln(\theta/(1-\theta))=f(\ln C)$. The corrosion rate decreased with the addition of 1,3-DPTA due to the formation of a hydrophobic film. This process is proven by measuring the contact angles of water after the samples are immersed in aggressive media with inhibitor for 24 hours. The hydrophobization of the steel surface increases with increase in the inhibitor concentration.

Received: November 1, 2023. Published: December 14, 2023 doi: 10.17675/2305-6894-2023-12-4-48

Keywords: *mild steel, acid corrosion inhibitor, thiadiazole, potentiodynamic polarization, contact angle, surface energy, electrochemical impedance, adsorption.*

Introduction

Corrosion of metals is a highly undesirable process since it damages metallic materials leading to their continuous destruction. Hydrochloric acid has important technical applications in such areas as acid etching, acid scale removal and acidification of oil wells. During these processes, the metal surface undergoes acid corrosion [1–3]. Consequently, various types of anticorrosive methods have been developed, including ones which prevent the contact of the material with the corrosive environment. Organic heterocyclic molecules can be adsorbed on the metal surface and form a protective film, thereby acting as corrosion inhibitors [4]. When the inhibitor is adsorbed on the steel surface, its electrochemical parameters and the wettability change. For better corrosion protection the steel surface should have hydrophobic properties in contact with aggressive media. The contact angle

measurement is sensitive to physical and chemical conditions at the solid-liquid interface [5]. The contact angle can be used both to determine the hydrophobicity of the inhibitor film and to calculate its adsorption on the steel surface [6–9].

In this article, traditional electrochemical methods and surface research methods were used to establish the adsorption parameters of 1,3-DPTA molecules on the steel surface.

Experimental Details

Synthesis

1,3-DPTA was chosen as inhibitor for the research. Since the previously obtained 2-amino-1,3,4-thiadiazoles showed good inhibitory properties [10], structural modifications were carried out, for which 2-amino-5-phenyl-1,3,4-thiadiazole was obtained by the interaction of benzoic acid and thiosemicarbazide in a $POCl_3$ medium (Scheme 1).

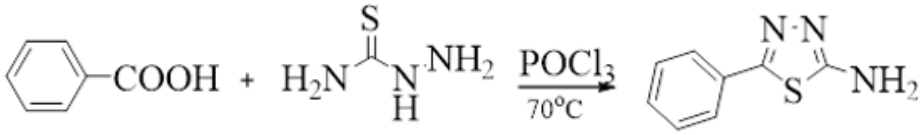

Scheme 1. Preparation of 2-amino-5-phenyl-1,3,4-thiadiazole.

Further, aromatic 2-amino-5-phenyl-1,3,4-thiadiazole interact with CS_2 and dibromoethane in the presence of a concentrated aqueous NaOH solution leads to the formation of 1,3-DPTA as a result of cyclization of the sodium salt of carbomoyl dithiolic acid (Scheme 2).

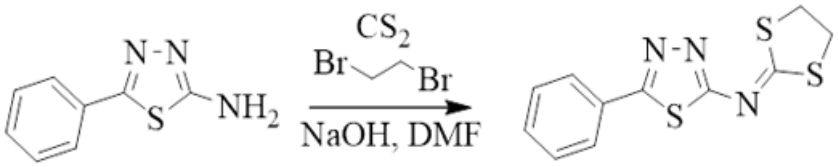

Scheme 2. Preparation of 1,3-DPTA.

Steel samples for experiments were made from mild steel St3 with the composition, wt.%: Fe–98.27; C–0.20; Mn–0.50; Si–0.30; P–0.04; S–0.04; Cr–0.15; Ni–0.30; Cu–0.20. The experiments were carried out in 1 M HCl solutions prepared from distilled water and 37% HCl.

NMR spectra of 1,3-DPTA: ^{1}H NMR (400 MHz, $CDCl_3$), δ, ppm: 7.94–7.92 (m, 2H), 7.47–7.42 (m, 3H), 3.71 (s, 2H), 3.58 (s, 2H); ^{13}C NMR (101 MHz, $CDCl_3$), δ, ppm: 182.81, 170.07, 166.55, 130.81, 130.89, 129.06, 127.50, 39.57, 34.99. Yield 62%.

Weight loss method

The weight loss method was used to calculate the corrosion rate (K) in grams per square meter per hour. The inhibition efficiency for each concentration of inhibitor was calculated according to the equation

$$IE(\%) = 1 - \frac{K_{inh}}{K_0} \times 100\%$$

where IE is the inhibition efficiency, K_{inh} and K_0 are the corrosion rate ($g \cdot m^{-2} \cdot h^{-1}$) with and without inhibitor, respectively.

Electrochemical measurements

A traditional three-electrode cell was used for electrochemical measurements. A platinum electrode was used for the auxiliary electrode, and the reference electrode was a silver chloride electrode (SCE) with a Luggin capillary. All potentials were measured with respect to the SCE. The working electrode is St3 mild steel electrode.

Before each experiment, all samples were mechanically polished with various grades of sandpaper (up to 2000 grit) and then cleaned in acetone, followed by rinsing in distilled water and drying.

Electrochemical experiments were carried out using electrochemical system Solatron 1280C. Potentiodynamic polarization curves were recorded at a sweep rate of 0.5 mV per 1 sec. Electrochemical impedance spectroscopy (EIS) measurements were carried out at open-circuit potential over a frequency range of 0.1–100 kHz. The sinusoidal potential perturbation was 5 mV in amplitude. Electrochemical data were obtained after 1 h of immersion with the working electrode at open-circuit potential. Electrochemical data were analyzed by Z-View software.

Based on the electrochemical results, the activation energy of the corrosion process was calculated. The calculations were performed by the temperature-kinetic method [11].

The surface coverage (θ) of the St3 electrode by inhibitor molecules was determined from the equation:

$$\theta = \frac{C_0 - C}{C_0 - C_1},$$

where C_0, C and C_1 are the capacitance of the double electric layer in the blank acid solution, in the solution with an inhibitor, and in the solution with $\theta=1$, respectively. The value of C_1 was determined by extrapolating the curve in the coordinates $1/C = f(1/C_{inh})$ to $(1/C_{inh})=0$, where C_{inh} is the concentration of the inhibitor in the solution, mg/L.

All the data presented in this work were obtained by averaging the results of three parallel measurements.

Sessile drop measurements

The contact angle and surface tension measurements were carried out using a tensiometer DSA 25E (KRUSS) by the sessile drop and pendant drop methods respectively [12]. The inhibitor solution in 1 M HCl was applied to the surface of mild steel. The volume of liquids was 1–2 ml.

Results and Discussion

IE (%) obtained from weight loss measurements for different concentrations of 1,3-DPTA for 24 hours in 1 M HCl were given in Figure 1. It could be seen that the 1,3-DPTA had tendency to increase *IE* (%) with increase concentration. Moreover, *IE* in the concentration range of 50–200 mg/l increased more slowly than at the beginning of the interval. If inhibition efficiency of 2-amino-5-phenyl-1,3,4-thiadiazole is compared with *IE* of 1,3-DPTA, then there is an increase in inhibition efficiency from 41 % to 83 %, respectively. That is, in order to increase the inhibition efficiency, modification of the amino group of the thiadiazole ring was carried out, which also led to improvement of surface active properties of the studied molecule in hydrochloric acid solutions.

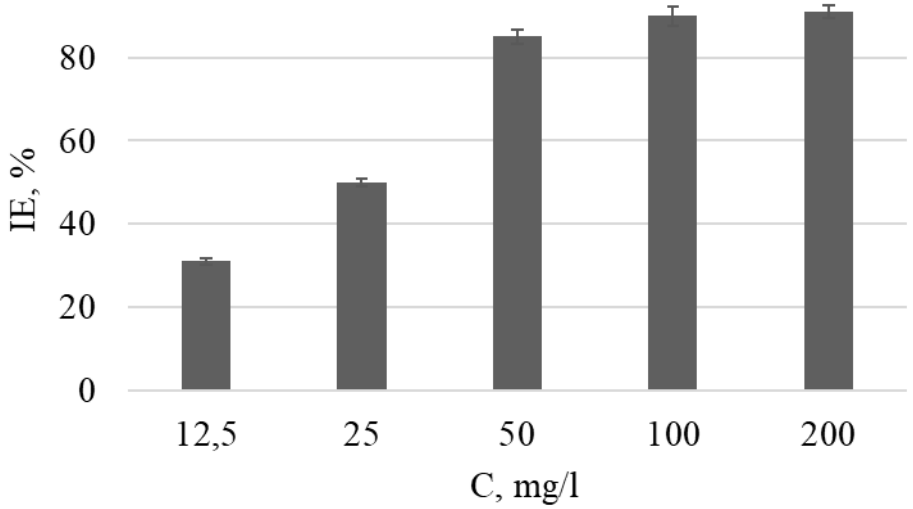

Figure 1. Inhibition efficiency (IE (%)) with different concentration of 1,3-DPTA for mild steel corrosion in 1 M HCl solution obtained by weight loss method.

Polarization curves for mild steel in 1 M HCl with 100 mg/l 1,3-DPTA were shown in Figure 2. The compound is a cathodic type inhibitor, since its introduction reduces the rate of cathodic process predominantly and does not affect anodic electrochemical process (Figure 2). The anodic and cathodic current–potential curves were extrapolated up to their intersection at the point where corrosion current density (i_{corr}) and corrosion potential (E_{corr}) were obtained, these results are presented in Table 1. According to the results presented, the free corrosion potential does not shift when an inhibitor is introduced into a corrosive environment up to a temperature of 333 K, and at a temperature of 353 K, a shift of the

corrosion potential to the cathode region by 60 mV is observed and *IE* increases to 88%. This may be due to the fact that with increasing temperature, the amount of the protonated form of the inhibitor molecule increases compared to the non-protonated form, and the protonated form is able to block the negatively charged steel surface during cathodic polarization.

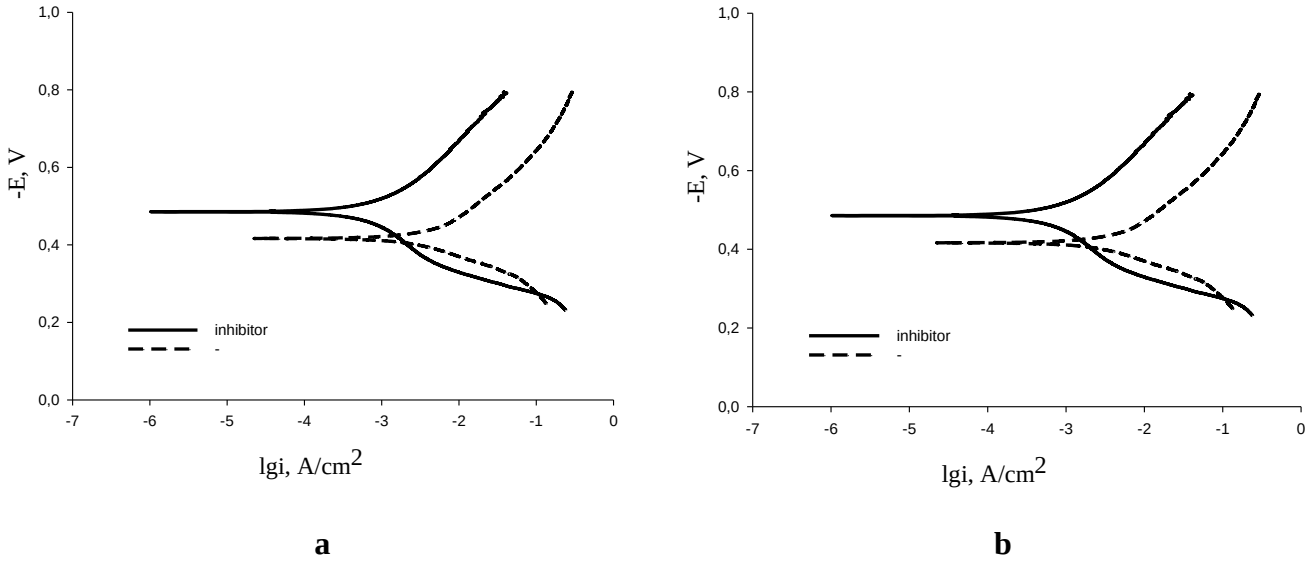

Figure 2. Polarization curves of mild steel in 1 M HCl containing 100 mg/L of 1,3-DPTA at 293 K (a) and at 353 K (b).

The activation energy of corrosion process can be obtained by investigating the influence of temperature on corrosion inhibition, consequently some information about adsorption mechanism of the inhibitor can be obtained from the activation energy values. In order to calculate the activation energy of the corrosion process, Arrhenius equation was used as

$$i_{\text{corr}} = k \exp\left(-\frac{E_{\text{a}}}{RT}\right),$$

where k is the pre-exponential factor, and E_{a} is the activation energy of the corrosion process. The Arrhenius plots of the natural logarithm of the corrosion current density *vs.* $1/T$ in the presence of 1,3-DPTA is $y = 1.6432x - 1.5257$, $R^2 = 0.978$, consequently E_{a} equals 13.7 kJ/mol compared to the blank solution where it is 42.9 kJ/mol [11]. The inspection of results shows that the value of E_{a} obtained in 1.0 M HCl containing 1,3-DPTA is lower than that obtained without inhibitor, which may be interpreted as chemical adsorption [13].

The corrosion inhibiting property of 1,3-DPTA on St3 steel was also examined by electrochemical impedance spectroscopy (EIS) in order to confirm the above obtained results and to study the adsorption inhibition mechanism. Figure 3 presents the Nyquist diagrams of St3 steel obtained at open-circuit potential in 1 M HCl solution in the absence and

presence of 1,3-DPTA at concentrations range from 12.5 to 200 mg/l after 60 min of immersion at 293 K. As shown in Figure 3, we remark that when 1,3-DPTA is added to the HCl solution, the size of the impedance diagram increases as the concentration rises and consequently the inhibitory efficacy increases, due to the adsorption of inhibitor molecules on the metal surface. Figure 4 shows the electrical equivalent circuit scheme to model St3/1 M HCl interface which consists of a CPE, solution resistance (R_s) and R_p is the polarization resistance, where R_p includes charge transfer resistance (R_{ct}) and the resistance of inhibitor film formed on the metal surface in the presence of inhibitor and two R–C parts describe adsorption of intermediate of cathodic and anodic electrochemical processes.

Table 1. Corrosion-electrochemical characteristics of mild steel in 1 M hydrochloric acid solutions with concentrations containing none or 100 mg/L of the inhibitor at various temperatures.

Inhibitor	***T*, K**	$i_{corr}\cdot10^{-4}$, **A/cm²**	$-E_{corr}$, **V**	***IE*, %**
–	293	2.27±0.06	0.455±0.015	–
100 mg/L		0.73±0.04	0.439±0.022	67.8
–	303	2.88±0.11	0.469±0.012	–
100 mg/L		0.88±0.05	0.438±0.015	69.0
–	313	5.05±0.13	0.445±0.013	–
100 mg/L		1.65±0.06	0.453±0.010	67.3
–	333	8.91±0.10	0.444±0.020	–
100 mg/L		3.19±0.04	0.458±0.018	67.2
–	353	42.0±0.20	0.406±0.016	–
100 mg/L		5.22±0.11	0.466±0.011	88.0

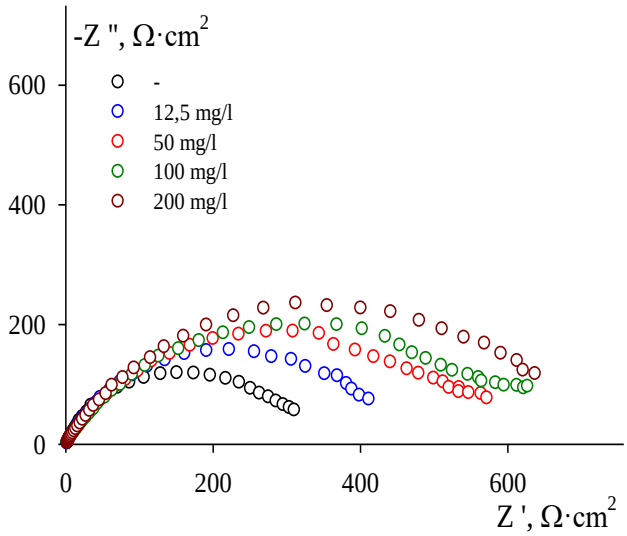

Figure 3. Nyquist impedance plot for mild steel in 1 M HCl solution in the absence and in the presence of different 1,3-DPTA concentrations.

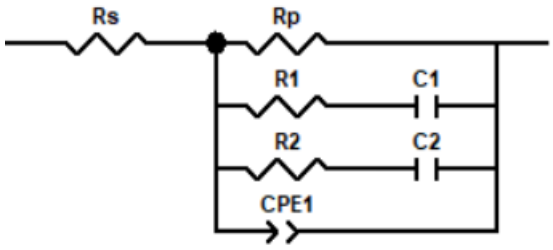

Figure 4. Equivalent electrical circuit for a mild steel electrode in 1 M HCl solutions at E_{corr}.

The capacitance of the double electric layer in the blank acid solution and in the solution with inhibitor from EIS measurements were calculated using equation:

$$C_{dl} = [Q(R_s^{-1} + R_{ct}^{-1})^{(p-1)}]^{1/p}$$

where R_s – resistance of solution; R_{ct} – resistance of electron charge transfer; Q and p are parameters of constant phase element CPE.

After that, the surface coverage (θ) of the St3 electrode by inhibitor molecules was calculated and plotted adsorption isotherms. The adsorption isotherms can provide basic information on the interaction of inhibitor and metal surface. In order to obtain adsorption isotherm, the surface coverage values (θ), for different concentrations of 1,3-DPTA in 1 M HCl solution have been obtained and tested graphically for fitting a suitable adsorption isotherm. Correlation coefficients for different type of isotherms were presented in Table 3. The plot of $\ln(\theta/(1-\theta))$ versus $\ln C_{inh}$ (Figure 5) yield a straight line with correlation coefficient of 0.972 and the slope of 2.118 providing that the adsorption of 1,3-DPTA in concentration range 12.5–200 mg/L on the mild steel surface obeys adsorption isotherm presented in [15]. If we consider a narrower concentration range of 25–100 mg/l, lnθ versus $\ln C_{inh}$ gives straight line with correlation coefficient of 0.9881 and adsorption behavior of the inhibitor on steel surface can be described by Freundlich equation. This type of adsorption isotherm is a special case of the Freundlich isotherm, which describes adsorption on energetically inhomogeneous surface, such as the steel surface under acid corrosion. The $\ln(\theta/(1-\theta)) = f(\ln C_{inh})$ isotherm expands the range of concentrations and involves, at low concentrations, adsorption by the local mechanism, *i.e.*, first of all, inhibitor molecules cover energetically more advantageous adsorption centers.

In the most general form, the solid–liquid interface adsorption from a dilute solution can be calculated based on the Gibbs equation:

$$\Gamma_{SL} = -\frac{1}{RT} \cdot \frac{\partial \gamma_{SL}}{\partial \ln C},$$

where Γ_{SL} is the surface concentration, *i.e.* the surface excess mass per unit area, γ_{SL} is the surface tension on the liquid–gas interface, and R and T have their usual meanings, C – inhibitor concentration.

In turn, the value of γ_{SL} can be determined based on the Young equation:

$$\gamma_{SG} = \gamma_{SL} + \gamma_{LG} \cos\theta,$$

where θ is the contact angle measured in the liquid, γ_{SG}, γ_{LG} and γ_{SL} are the surface tensions of solid, liquid, and solid-liquid surfaces.

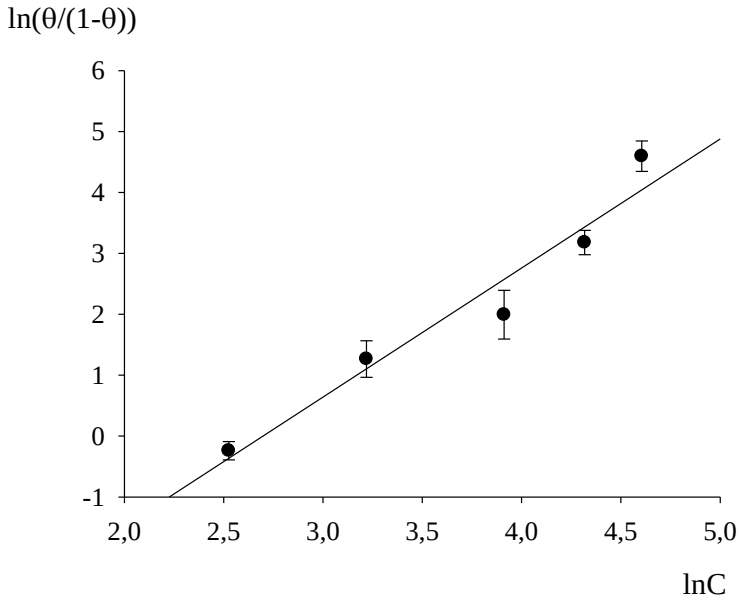

Figure 5. Adsorption plot for mild steel in 1 M HCl containing 1,3-DPTA.

When an inhibitor is introduced, the surface tension at the liquid-gas interface changes since our substance is surface active. Also, due to its adsorption on the steel surface, the contact angle changes, therefore the surface energy at the solid-gas interface is constant and adsorption can be calculated as:

$$\Gamma_{SL} = -\frac{1}{RT} \cdot \frac{\partial \gamma_{LG} \cdot \cos\theta}{\partial \ln C}$$

The concentration-dependent contact angles and concentration-dependent in coordinates $\gamma_{LG} \cos\theta = f(C)$ are shown in the Figure 6. The adsorption isotherms obtained by the contact angles method and by electrochemical impedance spectroscopy are compared below (Figure 7), the trend of isotherms is similar.

The differences in the dependencies of surface coverage (Figure 7) are due to the experimental conditions: the contact angles are measured “here and now”, and the impedance spectra are recorded after an immersion time of 1 hour.

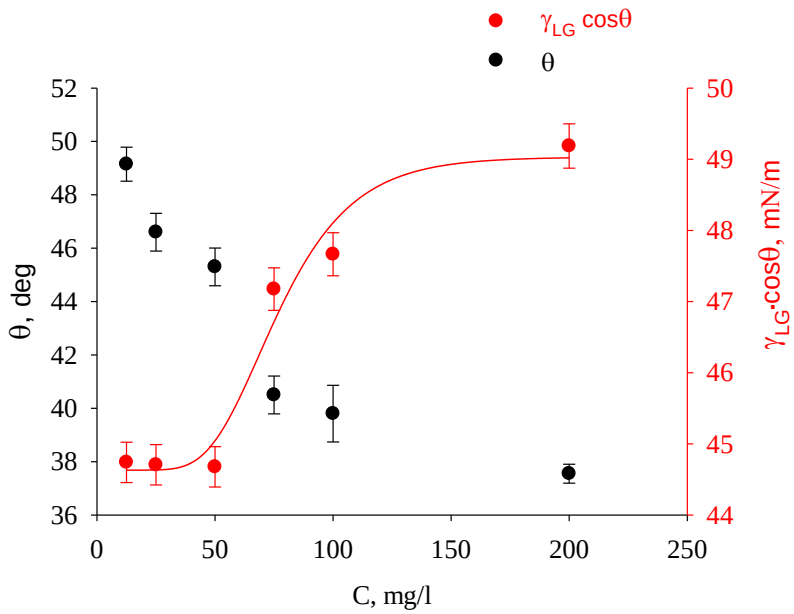

Figure 6. Variation of the contact angle (θ) and $\gamma_{LG}\cos\theta$ with different concentration of the inhibitor in 1 M HCl.

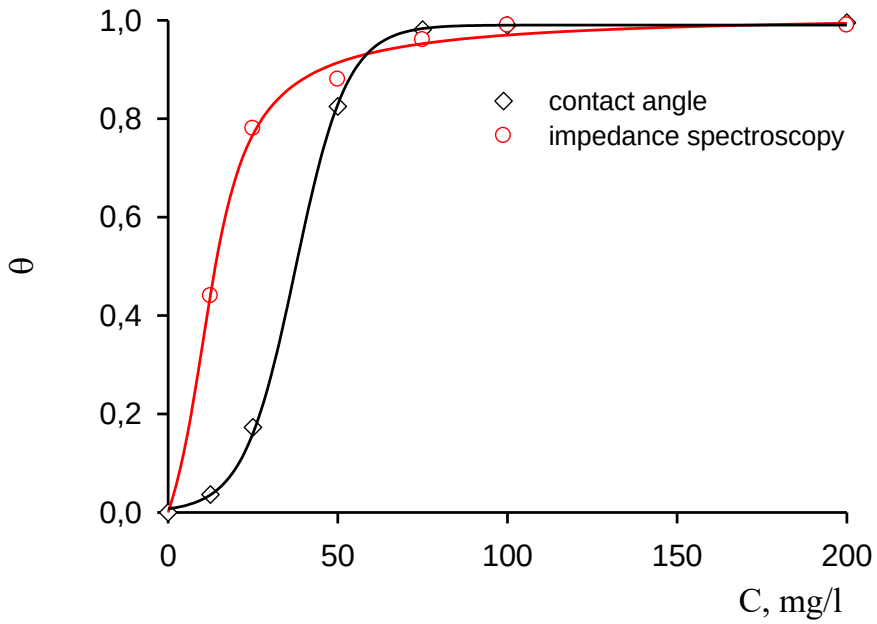

Figure 7. Dependence of surface coverage of mild steel in 1 M HCl with inhibitor concentration, obtained from contact angle (black line) and impedance spectroscopy (red line) data.

According to contact angle measurements protection film of inhibitor has hydrophobic properties as contact angles are 90 or more (Table 2).

Table 2. Contact angles of water after corrosion immersion during 24 hours.

Inhibitor concentration, mg·l^{-1}							
Test	Pure acid	12.5	25	50	75	100	200
							
Contact angle, deg							
94.8±1.4	42.2±1.6	68.9±1.7	81.0±11.7	86.5±2.4	92.7±0.2	92.7±0.5	92.1±2.3

In order to study the correlation between the adsorbent and adsorbate and to determine the best adopted presentation for the experimental data, we applied the adequate adsorption isotherms, namely Freundlich [16], Langmuir [17], Temkin [18, 19], Redlich–Peterson [20, 21], Zhang [15]. Their equations imply a linear relationship in coordinates presented in Table 3, where θ – surface coverage, C – inhibitor concentration.

The correlation coefficients of adsorption isotherm obtained based on the contact angels and impedance measurements are given in the Table 3. Similarly, the dependence obtained from the impedance spectroscopy results (Figure 5), the adsorption values calculated from the measurement of the contact angles are better linearized in coordinates:

$$\ln\frac{\theta}{1-\theta} = f(\ln C)$$

This model explains adsorption as a cooperative process and takes into account the local growth of the film, as well as the adsorption of half-micelles on steel surface, if the inhibitor has surface activity, as 1,3-DPTA.

Table 3. Correlation coefficients R^2 calculated for different adsorption models obtained by the two experimental methods: contact angel measurements and impedance spectroscopy.

Models	**Isotherms coordinates**	**Experimental method**	
		contact angle	**impedance**
Freundlich	$\ln\theta = f(\ln C)$	0.9704	0.8467
Langmuir	$\frac{C}{\theta} = f(C)$	0.5850	0.4691
Temkin	$\theta = f(\ln C)$	0.8530	0.9172
Redlich–Peterson	$\ln\frac{C}{\theta} = f(\ln C)$	0.9860	0.9517
[15]	$\ln\frac{\theta}{1-\theta} = f(\ln C)$	0.9950	0.9881

Conclusions

1. The results that were determined by weight loss method showed that the inhibition efficiency of 1,3-DPTA on the on the corrosion of mild steel in 1 M hydrochloric acid solutions is increased in concentration range from 12.5 to 50 mg/l (30–82%) and *IE* reaches 82–90% in concentration range from 50 to 200 mg/l. This effect is explained by the formation of a protective film of an organic inhibitor on the surface of corroding steel.
2. According to impedance spectroscopy and contact angle method surface coverage by molecules of inhibitor is 0.8 and more in same concentration range. 1,3-DPTA is a mixed-type inhibitor, but the free corrosion potential shifts to the cathode region with increasing temperature.
3. 1,3-DPTA has surface active properties and adsorbed on steel with forming hydrophobic protected film.
4. The type of adsorption isotherm of 1,3-DPTA obtained by the EIS method and the sessile drop method is a special case of the Freundlich isotherm explaining inhibitor adsorption as a cooperative process, taking into account the local growth of the film on energetically inhomogeneous surface and the aggregation of inhibitor molecules.

Acknowledgments

This research was supported by the Perm Scientific and Education Centre “Rational Subsoil Use”, 2023.

References

1. Yu.I. Kuznetsov, New possibilities of metal corrosion inhibition by organic heterocyclic compounds, *Int. J. Corros. Scale Inhib*., 2012, **1**, no. 1, 3–15. doi: 10.17675/2305-6894-2012-1-1-003-015
2. M.A. Deyab and Q. Mohsen, Inhibitory influence of cationic Gemini surfactant on the dissolution rate of N80 carbon steel in 15% HCl solution, *Sci. Rep*., 2021, **11**, 10521. doi: 10.1038/s41598-021-90031-x
3. T. Laabaissi, M. Rbaa, F. Benhiba, Z. Rouifi, U.P. Kumar, F. Bentiss, H. Oudda, B. Lakhrissi, I. Warad and A. Zarrouk, Insight into the corrosion inhibition of new benzodiazepine derivatives as highly efficient inhibitors for mild steel in 1 M HCl: Experimental and theoretical study, *Colloids Surf., A*, 2021, **629**, 127428. doi: 10.1016/j.colsurfa.2021.127428
4. M.D. Plotnikova, A.B. Shein, M.G. Shcherban and A.D. Solovyev, The study of thiadiazole derivatives as potential corrosion inhibitors of low-carbon steel in hydrochloric acid, *Bulletin of the University of Karaganda – Chemistry*, 2021, **103**, no. 3, 93–102. doi: 10.31489/2021Ch3/93-102

5. C.H. Kung, P.K. Sow, B. Zahiri and W. Mérida, Assessment and interpretation of surface wettability based on sessile droplet contact angle measurement: challenges and opportunities, *Adv. Mater. Interfaces*, 2019, **6**, no. 18, 1900839. doi: 10.1002/admi.201900839
6. U. Messow, P. Braeuer, A. Schmidt, C. Bilke-Krause, K. Quitzsch and U. Zilles, Calculation of adsorption isotherms on hard solid surfaces using measurements of surface tensions and contact angles, *Adsorption*, 1998, **4**, 257–267. doi: 10.1023/A:1008833700390
7. E.A. Vogler, Practical use of concentration-dependent contact angles as a measure of solid-liquid adsorption. 1. Theoretical aspects, *Langmuir*, 1992, **8**, no. 8, 2005–2012. doi: 10.1021/la00044a022
8. E.A. Vogler, Practical use of concentration-dependent contact angles as a measure of solid-liquid adsorption. 2. Experimental aspects, *Langmuir*, 1992, **8**, no. 8, 2013–2020. doi: 10.1021/la00044a023
9. T.J. Horr, J. Ralston, R.St.C. Smart, The use of contact angle measurements to quantify the adsorption density and thickness of organic molecules on hydrophilic surfaces, *Colloids Surf., A*, 1995, **97**, no. 3, 183–196. doi: 10.1016/0927-7757(95)03090-Z
10. M.D. Plotnikova, A.D. Solovyev, A.B. Shein, A.N. Vasyanin and A.S. Sofronov, Corrosion inhibition of mild steel by triazole and thiadiazole derivatives in 5 M hydrochloric acid medium, *Int. J. Corros. Scale Inhib*., 2021, **9**, no. 3, 1336–1354. doi: 10.17675/2305-6894-2021-10-3-29
11. M.D. Plotnikova, A.D. Shitoeva, A.D. Solovyev, A.N. Bakiev and A.B. Shein, Some aspects of the of the mechanism of C1018 steel protection in hydrochloric acid solutions by triazole derivatives, *Int. J. Corros. Scale Inhib*, 2023, **12**, no. 2, 511–530. doi: 10.17675/2305-6894-2023-12-2-8
12. R.S. Hebbar, A.M. Isloor and A.F. Ismail, Chapter 12 – Contact Angle Measurements, *Membrane Characterization*, Elsevier, 2017, pp. 219–255. doi: 10.1016/B978-0-444-63776-5.00012-7
13. A.K. Singh and M.A. Quraishi, The effect of some bis-thiadiazole derivatives on the corrosion of mild steel in hydrochloric acid, *Corros. Sci*., 2010, **52**, no. 4, 1373–1385. doi: 10.1016/j.corsci.2010.01.007
14. Y. Tang, X. Yang, W. Yang, Y. Chen and R. Wan, Experimental and molecular dynamics studies on corrosion inhibition of mild steel by 2-amino-5-phenyl-1,3,4-thiadiazole, *Corros. Sci*., 2010, **52**, no. 1, 242–249. doi: 10.1016/j.corsci.2009.09.010
15. R. Zhang, C. Liu and P. Somasundaran, A model for the cooperative adsorption of surfactant mixtures on solid surfaces, *J. Colloid Interface Sci*., 2007, **310**, no. 2, 377–384. doi: 10.1016/j.jcis.2007.01.099
16. H. Freundlich, Über die Adsorption in Lösungen (About the adsorption in solutions), *Z. Phys. Chem. (Berlin, Ger.)*, 1907, **57**, 385–470 (in German). doi: 10.1515/zpch-1907-5723

17. I. Langmuir, The adsorption of gases on plane surfaces of glass, mica and platinum, *J. Am. Chem. Soc*., 1918, **40**, no. 9, 1361–1403. doi: 10.1021/ja02242a004
18. M.V. Vigdorovich, L.E. Cygankova and N.V. Shel', Polilogarifmicheskaya izoterma adsorbcii pri linejnoj energeticheskoj neodnorodnosti poverhnosti (Polylogarithmic adsorption isotherm with linear energy inhomogeneity of the surface), *Vestnik Nacional'nogo Issledovatel'skogo Yadernogo Universiteta MIFI (Bulletin of the National Research Nuclear University MIFI)*, 2020, **9**, no. 5, 389–395 (in Russian). doi: 10.1134/S2304487X20050156
19. L.E. Cygankova, N. Al'shikha, M.V. Vigdorovich and I.V. Zarapina, Analiz adsorbcii ingibitora korrozii uglerodistoj stali v model'nyh plastovyh vodah posredstvom polilogarifmicheskoj izotermy (Analysis of adsorption of carbon steel corrosion inhibitor in model reservoir waters by means of polylogarithmic isotherm), *Korroz.: Mater., Zashch. (Corrosion: Materials, Protection)*, 2021, **1**, 20–26 (in Russian). doi: 10.31044/1813-7016-2021-0-1-20-26
20. F.-C. Wu, B.-L. Liu, K.-T. Wu and R.-L. Tseng, A new linear form analysis of Redlich–Peterson isotherm equation for the adsorptions of dyes, *Chem. Eng. J*., 2010, **162**, no. 1, 21–27. doi: 10.1016/j.cej.2010.03.006
21. V. Kumar and S. Sivanesan, Prediction of optimum sorption isotherm: Comparison of linear and non-linear method, *J. Hazard. Mater*., 2005, **126**, no. 1–3, 198–201. doi: 10.1016/j.jhazmat.2005.06.007

♦ ♦ ♦